Research Square

Preprints are preliminary reports that have not undergone peer review.
They should not be considered conclusive, used to inform clinical practice,
or referenced by the media as validated information.

Evaluation of Coal Spontaneous Combustion (CSC) Liability Based on Particle Size Distribution (PSD) and Specific Surface Area (SSA)

Serdar YILMAZ

serdaryilmaz@beun.edu.tr

Zonguldak Bülent Ecevit University

Mehmet BİLEN

Zonguldak Bülent Ecevit University

Kemal BARIŞ

Zonguldak Bülent Ecevit University

Research Article

Keywords: Coal spontaneous combustion (CSC), Particle size distribution (PSD), Specific surface area (SSA), Coal oxidation, Thermal reactivity

Posted Date: August 24th, 2026

DOI: https://doi.org/10.21203/rs.3.rs-10395316/v1

License: This work is licensed under a Creative Commons Attribution 4.0 International License.
Read Full License

Additional Declarations: No competing interests reported.

Evaluation of Coal Spontaneous Combustion (CSC) Liability Based on Particle Size Distribution (PSD) and Specific Surface Area (SSA)

Serdar YILMAZ[1*], Mehmet BİLEN[1], Kemal BARIŞ[2]

[1]Department of Mining Engineering, Zonguldak Bülent Ecevit University,
67100, Zonguldak, TÜRKİYE

[2]Department of Mining and Mineral Extraction, Zonguldak Bülent Ecevit University, Kilimli
67500, Zonguldak, TÜRKİYE

serdaryilmaz@beun.edu.tr

*Corresponding author

Abstract

Coal spontaneous combustion (CSC) remains one of the most critical safety concerns in coal mining operations, and its reliable assessment requires robust indicators capable of capturing the complex interplay between coal particle characteristics and oxidation behavior. In this study, a comprehensive experimental investigation was conducted on 216 coal samples to systematically evaluate the relationships between particle size distribution (PSD), specific surface area (SSA), and spontaneous combustion liability. Accordingly, for each sample, detailed PSD parameters including D10, D50, D90, D32, and D43, together with SSA values, were experimentally determined in order to characterize the particle-scale physical structure with high resolution and consistency. In parallel, the spontaneous combustion propensity of the same coal samples was quantified using three widely accepted indices, namely the Flammability Characteristic Constant (FCC), Crossing Point Temperature (CPT), and Average Temperature Increase (ATI), thereby enabling a comprehensive evaluation of coal oxidation

behavior under controlled conditions. Furthermore, the coal samples used in the CPT experiments were carefully pulverized and standardized to ensure uniform particle size conditions, which allowed a systematic and reproducible assessment of the influence of PSD and SSA variations on thermal reactivity. Subsequently, correlation analyses were performed to investigate the relationships between particle-scale parameters and combustion liability indicators, where PSD and SSA metrics were directly compared with FCC, CPT, and ATI values. The obtained results consistently demonstrate strong and statistically meaningful relationships between coal physical properties and spontaneous combustion behavior. In particular, finer particle fractions reflected by lower D10, D50, and D90 values, as well as higher surface complexity indicated by D32, D43, and elevated SSA levels, were found to be strongly associated with increased oxidation reactivity, reduced thermal stability, and higher spontaneous combustion liability. Consequently, these findings clearly indicate that both particle size distribution and specific surface area serve as fundamental controlling factors governing coal–oxygen interaction dynamics, and therefore provide a reliable and practical framework for the prediction and assessment of spontaneous combustion risk in coal materials under industrial mining conditions.

Keywords: Coal spontaneous combustion (CSC); Particle size distribution (PSD); Specific surface area (SSA); Coal oxidation; Thermal reactivity

1. Introduction

Coal spontaneous combustion (CSC) persistently remains one of the most intractable and technically challenging safety hazards confronting both underground and surface mining operations across the globe. Indeed, despite remarkable advancements in mine ventilation engineering, real-time atmospheric monitoring systems, and state-of-the-art fire suppression

technologies over recent decades, the complete elimination of this peril has proven elusive. Consequently, it continues to inflict substantial economic losses through equipment damage and production disruptions, causes significant environmental degradation due to greenhouse gas and toxic fume emissions, and, most critically, poses an ever-present and serious threat to the health and safety of mine workers. At its core, this phenomenon originates from low-temperature exothermic reactions that initiate when coal is exposed to atmospheric oxygen over extended periods. During this process, the heat generated by chemisorption and subsequent oxidation may accumulate within the coal mass at a rate exceeding its dissipation to the surrounding strata or ventilated air currents. Should this thermal imbalance persist, it leads progressively to self-heating and, provided that favorable oxygen availability and thermal insulation conditions are met, culminates in spontaneous ignition. However, it is crucial to recognize that the onset, evolution, and ultimate severity of spontaneous combustion are governed by a highly intricate and nonlinear interplay of physical properties (such as porosity and thermal conductivity), chemical composition (including rank, functional groups, and mineral matter), and environmental variables (namely moisture content, ambient temperature, and airflow patterns). This multifactorial complexity renders accurate prediction and reliable risk assessment exceptionally difficult. For this reason, a comprehensive understanding of the fundamental parameters that control coal oxidation behavior continues to represent a critical research priority, not only for the scientific community but also for operational decision-making in the mining industry.

Among the numerous factors that influence spontaneous combustion susceptibility, particle size has long been acknowledged as one of the most decisive parameters, primarily because it directly governs the specific surface area available for oxygen adsorption and subsequent chemical reaction. In essence, as coal particles become progressively finer, the exposed reactive

surface area per unit mass increases considerably. This enhancement, in turn, facilitates more rapid oxygen diffusion into the particle interior, amplifies the adsorption capacity, and increases the collision frequency between oxygen molecules and reactive sites, thereby accelerating the overall oxidation kinetics. In modern mechanized mining operations—which involve extraction, crushing, grinding, conveying, and stockpiling—substantial quantities of fine coal particles are inevitably generated. This abundance of fines significantly elevates the spontaneous heating risk throughout the production chain. Since oxidation reactions occur predominantly at the coal surface, reductions in particle size generally translate into accelerated oxidation rates, intensified heat release, and consequently, lower ignition temperatures. Moreover, particle size is not merely a surface-related attribute; it also profoundly influences the internal pore architecture, porosity distribution, and accessibility of embedded reactive functional groups. These structural modifications, in turn, affect the overall oxidation kinetics and thermal behavior in a more indirect yet equally important manner (Wang et al., 2023; Du et al., 2023; Mishra et al., 2025). Therefore, particle-size-related characteristics are widely regarded as indispensable physical indicators for evaluating spontaneous combustion proneness, and they have thus become a focal point in many hazard assessment protocols.

Over the years, a considerable body of experimental research has convincingly demonstrated the strong and systematic relationship between particle size and coal oxidation behavior. For instance, in some of the earlier foundational studies, Jiang et al. (1999), Zhang et al. (2011), and Yu et al. (2016) consistently reported that decreasing particle size enhances oxygen adsorption capacity and oxygen consumption rates, thereby accelerating low-temperature oxidation processes. In a similar vein, Yang et al. (2019) showed, through advanced spectroscopic analyses, that particle size affects not only the macroscopic reaction rates but also the evolution of the coal's internal chemical structure, particularly the concentration of free

radicals and the distribution of oxygen-containing functional groups such as carboxyl, hydroxyl, and carbonyl moieties. Likewise, Qin et al. (2010) observed that coal samples with particle sizes in the range of 0 to 0.9 mm exhibit significantly higher oxidation rates compared to coarser fractions, thus providing direct empirical confirmation of the critical role played by particle fineness. More recently, Li et al. (2020) and Mishra et al. (2025) have further emphasized that finer particles, by virtue of their larger specific surface area, create more favorable conditions for oxygen diffusion and adsorption, which consequently result in enhanced self-heating tendencies and increased spontaneous combustion liability. Collectively, these findings strongly suggest that particle size distribution is far more than a mere physical attribute; rather, it represents a fundamental control parameter that modulates oxidation reactivity and thermal response at multiple scales.

Nevertheless, it must be stressed that the influence of particle size on spontaneous combustion is not always straightforward or monotonic. In fact, several studies have revealed that this relationship may exhibit threshold effects, depending critically on coal rank, mineral composition, pore structure, and prevailing environmental conditions. For example, Wang et al. (2016) observed that differences in ignition temperature become statistically insignificant when particle sizes drop below approximately 0.2 mm, suggesting that oxidation behavior may reach a saturation point at very fine particle sizes—likely due to diffusional limitations or changes in the dominant reaction mechanism. Similarly, Zhang et al. (2014) demonstrated that the combined and synergistic effects of particle size, porosity, and specific surface area exert a strong influence on heat accumulation and temperature rise during the oxidation process. Furthermore, Mishra et al. (2025) highlighted that spontaneous heating behavior is also modulated by geological and operational variables, including seam depth, extraction method, and residual coal distribution in goaf areas. These observations collectively imply that particle

size alone cannot sufficiently explain the full complexity of spontaneous combustion behavior; instead, additional parameters related to surface characteristics, such as specific surface area, pore volume, and surface roughness, must be taken into account for a more holistic risk assessment.

In recent decades, substantial progress has been achieved in the development of both laboratory-based and field-applicable methodologies for evaluating spontaneous combustion liability. To this end, numerous researchers have employed a diverse array of experimental testing protocols, extended field observations, and sophisticated numerical simulations to investigate the evolution of coal oxidation and self-heating processes (Onifade and Genc, 2020; Wolf and Bruining, 2007; Taraba et al., 2014). As a direct outcome of these concerted efforts, several quantitative indicators have been proposed for assessing spontaneous combustion risk. These include, but are not limited to, oxygen consumption rates, characteristic gas generation ratios (particularly the CO-to-CO_2 index), apparent activation energy, thermal diffusivity, and various combustion threshold indices. For instance, Kong et al. (2019), Deng et al. (2018), Qin et al. (2012), Wen et al. (2017), and Yong et al. (2019) have each developed distinct experimental approaches to characterize coal oxidation behavior and to quantify spontaneous combustion propensity from different methodological perspectives. In addition, complementary studies have examined the influence of coal rank, methane concentration, heat release intensity, thermophysical properties, and oxidation kinetics on the overall spontaneous combustion characteristics (Wang et al., 2021; Ma et al., 2018; Yang et al., 2018). Although these investigations have collectively and significantly improved our current understanding, it is noteworthy that the vast majority of these studies have predominantly focused on gas generation behavior, oxidation kinetics, and environmental drivers. By contrast, comparatively fewer studies have systematically explored how detailed particle size distribution (PSD)

characteristics and specific surface area (SSA) jointly and quantitatively influence the established spontaneous combustion liability indices, thereby leaving a notable gap in the existing literature.

Despite the considerable progress achieved in the development of spontaneous combustion assessment methodologies, a fundamental challenge remains associated with the practical monitoring and characterization of coal self-heating processes. Although direct measurement of coal temperature within coal seams, stockpiles, or goaf areas is generally regarded as one of the most reliable approaches for evaluating spontaneous combustion risk, obtaining accurate in-situ temperature data is often difficult due to limited accessibility, heterogeneous geological conditions, ventilation effects, and sensor deployment constraints (Choi et al., 2011). Consequently, laboratory-based experimental systems have become indispensable tools for investigating coal oxidation behavior under controlled conditions. Over the past decade, numerous researchers have developed specialized experimental platforms, including programmed heating systems, low-temperature oxidation reactors, and large-scale spontaneous combustion furnaces, to reproduce the self-heating process and identify characteristic indicators associated with spontaneous combustion liability. For example, Deng et al. (2015) constructed a 15-ton experimental furnace capable of continuously monitoring temperature evolution, oxygen depletion, and gaseous product generation during spontaneous combustion. Similarly, Zhang et al. (2019) combined FTIR spectroscopy with a programmed heating system to examine both molecular structural transformations and macroscopic oxidation characteristics, while Du et al. (2020) and Qin et al. (2020) employed temperature-programmed oxidation experiments to quantify oxygen consumption behavior and characterize oxidation kinetics under controlled laboratory conditions. These studies have substantially improved the

understanding of coal oxidation mechanisms and have provided valuable indicators for spontaneous combustion prediction.

At the same time, extensive research has demonstrated that coal oxidation behavior is highly sensitive to variations in intrinsic coal properties and external environmental conditions. Parameters such as coal rank, moisture content, oxygen availability, mineral composition, and particularly particle size have been repeatedly identified as major factors governing spontaneous combustion susceptibility (Küçük et al., 2003; Arisoy and Beamish, 2015; Zhou et al., 2020). During mining, transportation, crushing, and handling operations, coal is fragmented into particles of varying sizes, thereby creating fresh reactive surfaces that significantly increase the probability of coal–oxygen interactions (Zhang and Zhang, 2019; Xu et al., 2021). From a mechanistic perspective, particle size reduction leads to an increase in specific surface area, which enhances oxygen diffusion and adsorption while simultaneously lowering the apparent energy barrier required for oxidation reactions. As a result, finer particles generally exhibit higher oxidation rates and stronger self-heating tendencies than coarser fractions. Supporting this interpretation, Li et al. (2019) reported that the activity and thermal response of hydroxyl radicals decrease with increasing particle size, indicating diminished oxidation reactivity in larger particles. Likewise, Zhao et al. (2019) demonstrated significant variations in oxygen consumption characteristics among coal samples with different particle sizes, whereas Song et al. (2021a) identified critical particle size thresholds governing oxidation behavior during high-temperature heating experiments. Furthermore, Nugroho et al. (2000) observed that the relationship between particle size and spontaneous heating differs according to coal rank, suggesting that particle-scale effects may vary considerably among coal types.

Nevertheless, despite the growing recognition of particle size as a critical factor influencing spontaneous combustion behavior, current knowledge remains fragmented regarding the quantitative influence of particle size distribution characteristics and specific surface area on spontaneous combustion liability. Most previous investigations have focused on individual particle size fractions, oxygen consumption behavior, gas generation characteristics, or activation energy calculations, while relatively few studies have systematically examined the combined influence of detailed PSD descriptors and SSA parameters on widely accepted spontaneous combustion indices. In practical mining environments, residual coal accumulations are composed of highly heterogeneous particle size mixtures rather than uniform fractions, resulting in substantial variability in oxidation activity, oxygen uptake capacity, and heat generation behavior. Consequently, evaluating spontaneous combustion risk solely on the basis of isolated particle size classes may not adequately represent the complex conditions encountered in real mining operations. Moreover, although the Arrhenius relationship between oxidation rate and temperature has been widely utilized to derive apparent activation energy as an indicator of spontaneous combustion propensity (Deng et al., 2019; Song et al., 2021b), the extent to which PSD-related parameters and specific surface area collectively influence established liability indices remains insufficiently understood. This limitation highlights a significant gap in the current literature and underscores the need for comprehensive studies that directly integrate particle-scale physical characteristics with spontaneous combustion assessment parameters.

Recent studies have further highlighted the critical role of particle size distribution and specific surface area in governing coal oxidation and spontaneous combustion behavior. For example, Mishra (2022) demonstrated that decreasing coal particle size significantly increases specific surface area and enhances spontaneous combustion susceptibility by promoting oxygen

adsorption and coal–oxygen interactions. Their findings revealed a strong inverse relationship between particle size and SSA, while also identifying a critical particle size range below which further size reduction has little influence on oxidation rates. Moreover, the authors emphasized that spontaneous combustion is controlled by a complex interplay among particle size, surface area, coal composition, moisture content, and gas adsorption behavior. As illustrated in Figure 1, the spontaneous combustion process involves successive stages of oxygen adsorption, coal–oxygen complex formation, heat generation, and heat accumulation, ultimately leading to self-heating and ignition.

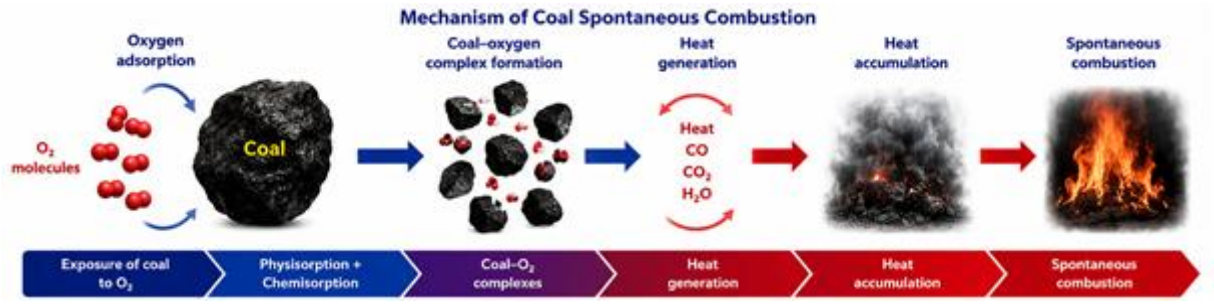


Figure 1. Schematic of the coal spontaneous combustion process and its key stages, adapted and modified from the study of Mishra (2022).

In this context, the present study aims to fill this gap by investigating a comprehensive and robust dataset comprising 216 coal samples, with the overarching goal of evaluating the interrelationships between particle size distribution (PSD), specific surface area (SSA), and spontaneous combustion liability. To achieve this objective, detailed PSD parameters—including D10, D50, D90, D32, and D43—along with SSA values were experimentally determined for each sample to systematically characterize their particle-scale physical attributes. In parallel, spontaneous combustion susceptibility was assessed using three widely accepted and complementary liability indices, namely the Flammability Characteristic Constant (FCC), Crossing Point Temperature (CPT), and Average Temperature Increase (ATI). Notably,

the pulverized coal samples employed in the CPT experiments were also subjected to comprehensive PSD and SSA analyses, thereby enabling a direct and rigorous examination of the relationships between particle-scale properties and combustion behavior. Through extensive statistical and correlation analyses—including Pearson correlation, multivariate regression, and sensitivity assessments—this study endeavors to: (i) quantitatively elucidate the influence of PSD and SSA on FCC, CPT, and ATI values; (ii) identify the most sensitive and statistically significant particle-related indicators that govern spontaneous combustion behavior; and (iii) establish a more robust, multi-parameter analytical framework for evaluating and predicting CSC risk under realistic mining and coal-processing conditions. Ultimately, the findings of this research are expected to provide both theoretical insights and practical guidance for enhancing early-warning systems and fire prevention strategies in the coal industry.

2. Material and Method

2.1. Sample Description and Methodology

2.1.1. Sampe Description

In this study, a comprehensive dataset consisting of 216 coal samples was utilized to investigate the relationships between particle size distribution (PSD), specific surface area (SSA), and coal spontaneous combustion (CSC) liability. The analyzed samples represent a wide range of coal characteristics, geological conditions, and coal ranks, including coals obtained from major Turkish coalfields, particularly the Zonguldak Basin (Bağlık–İnağzı and Karadon), as well as imported steam coals previously characterized in the literature (Bilen 2025, Yılmaz 2025, Bilen et al., 2026). It should be noted that the coal samples investigated in the present study are identical to those previously employed by Bilen et al. (2026) for RGB and color-space-based image analysis investigations. Building upon that dataset, the current research extends the characterization framework by determining the particle size distribution (PSD) parameters and

specific surface area (SSA) values of the same coal samples and subsequently evaluating their relationships with established spontaneous combustion liability indices. This approach enables the direct integration of particle-scale physical properties with spontaneous combustion behavior, thereby providing a more comprehensive understanding of the factors controlling coal oxidation and self-heating tendencies.

2.1.1.1.Coal Samples from Different Regions of Türkiye (n = 101)

The first sample group consists of 101 coal samples collected from major coal-producing regions throughout Türkiye (Figure 2). These samples represent a wide spectrum of coal ranks and geological settings, providing a representative overview of the diversity of Turkish coal resources. Owing to their varying petrographic, mineralogical, and physicochemical properties, these samples constitute the principal dataset for evaluating the influence of PSD and SSA characteristics on spontaneous combustion liability. The inclusion of coals from multiple regions enables the assessment of regional variability and improves the robustness of the statistical relationships established in this study.

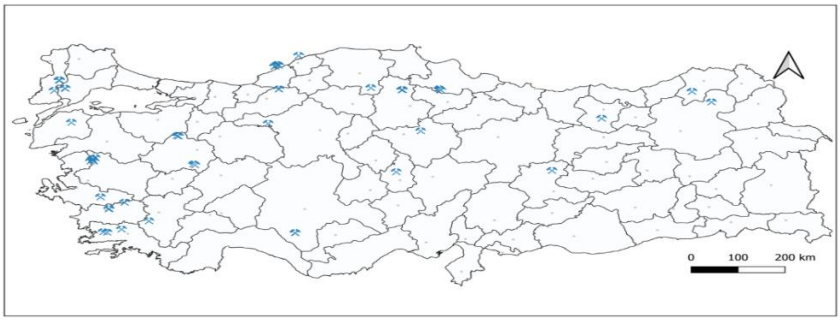


Figure 2. Spatial distribution of the sampling sites across major coal-producing regions of Türkiye.

2.1.1.2. Zonguldak Bağlık–İnağzı Drilling Core Coal Samples (n = 55)

The second sample group comprises 55 drilling core coal samples collected from the Bağlık–İnağzı sector of the Zonguldak Coal Basin. The samples were obtained from six different burial depths in order to capture vertical variations in coal characteristics associated with geological evolution and coalification processes. Prior to analysis, the samples were crushed to below 10 mm, and clay-rich fractions were removed through density separation using a medium density of 1.60 g/cm³. The floated fractions were subsequently washed, dried at 105 °C, and prepared for further characterization. These samples provide an important opportunity to investigate the influence of depth-related geological factors on PSD characteristics, SSA values, and spontaneous combustion liability indices.

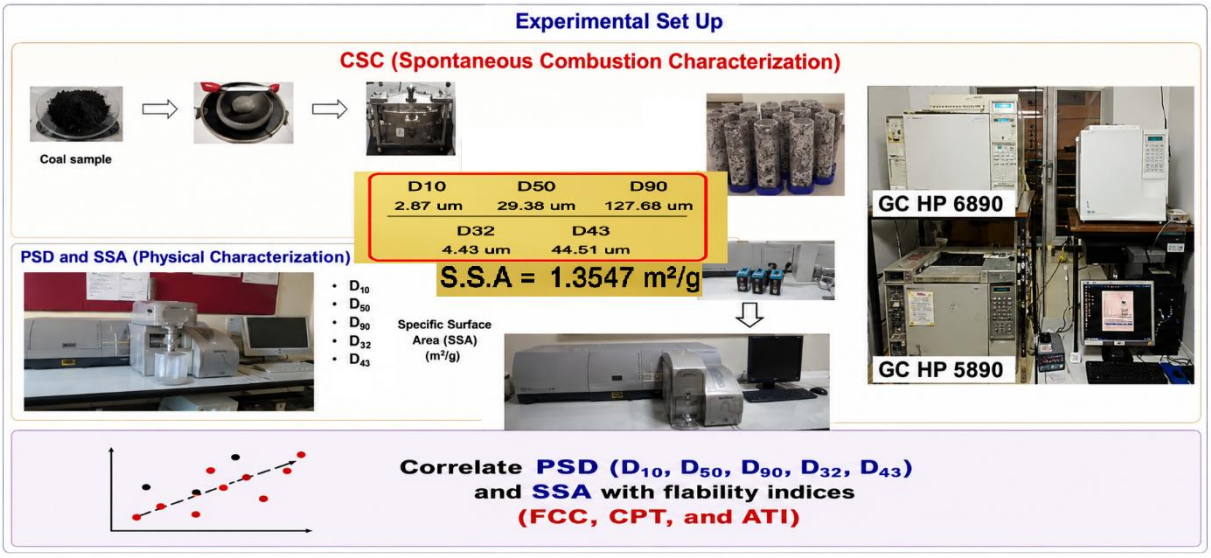
2.1.1.3. Zonguldak Karadon Region Coal Samples (n = 26)

The third dataset consists of 26 coal samples collected from the Karadon region of the Zonguldak Coal Basin. Detailed information regarding sampling procedures, sample preparation, and coal properties has previously been reported by Bilen (2025). The spontaneous combustion liability data generated in that study were incorporated into the present investigation, while PSD and SSA measurements were performed on the same sample set to establish relationships between particle-scale physical characteristics and combustion behavior. Due to the comprehensive characterization available for these samples, the Karadon dataset serves as a valuable reference group for validating the observed trends and strengthening comparative analyses among different coal populations.

2.1.1.4. Imported Steam Coal Samples (n = 34)

The final sample group includes 34 imported steam coal samples obtained from various international sources and previously characterized by Yılmaz (2025). These coals exhibit distinct geological origins, coalification histories, and compositional characteristics compared

317 with domestic Turkish coals, thereby expanding the variability of the overall dataset. The
318 inclusion of imported coals broadens the applicability of the study and allows the relationships
319 between PSD, SSA, and spontaneous combustion liability to be evaluated across a wider range
320 of coal types. Consequently, this dataset contributes to the development of more generalized
321 conclusions regarding the influence of PSD and SSA on CSCcombustion behavior.
322
323 **2.2. Methodology**
324 Methodology of this current research includes the PSD and SSA measurements of the samples
325 prepared for CSC liability tests. This PSD and SSA measurements carried out with employment
326 of Malvern Mastersizer S 2000 equipment (detailed information is provided in upcoming
327 sections). CSC liability tests were performed with a joint Gas Chromatograph laboratory. CSC
328 liability tests require coal samples to be milled under specific sieve size of 200 microns. But
329 the samples even though milled under this specific sieve size have mostly have different size
330 distribution graphs and so the size parameters and SSA values. To further investigate this effect
331 of PSD and SSA in terms of the CSC variation, same samples were subdivided into two groups,
332 i.e. one for physical characterization and the other for CSC liability characterization. In this
333 context, schematical representation of experimental methodology is provided in Figure 3.
334



335

336 **Figure 3.** Experimental methodology employed in the context of this study, previously PSD
337 and SSA measurements conducted by Yilmaz (2019), CSC experiments were conducted by
338 Bilen (2025).

339

340 **2.2.1. Particle Size Distribution (PSD) and Specific Surface Area (SSA) Experiments**

341 To investigate the influence of particle size physical properties on coal spontaneous combustion
342 (CSC) behavior, particle size distribution (PSD) and specific surface area (SSA) analyses were
343 conducted on the coal samples prepared for spontaneous combustion testing. Prior to the PSD
344 and SSA experiments, all samples (a total of 216) were grinded in accordance with the CSC
345 experimental procedure.

346

347 The particle size distribution (PSD) characteristics of the coal samples, which had been
348 previously ground in the order of CSC tests, were systematically analyzed by means of a
349 Malvern Mastersizer S 2000 laser diffraction instrument, employing the wet dispersion method
350 for all measurements. The operational detection range of the apparatus spanned from 0.05 µm
351 to as large as 878.67 µm, thereby ensuring comprehensive coverage of the entire particle size
352 spectrum of interest. For the purpose of accurate optical analysis, the refractive indices of the

dispersant (deionized water) and the coal particles were set to 1.33 and 1.64, respectively, in accordance with standard reference values. Throughout the measurement sequence, the obscuration parameter—which is a critical indicator of sample concentration—was carefully controlled and consistently maintained between 10% and 30%, with the majority of the tests being conducted at an obscuration level of approximately 20% to ensure optimal signal quality and measurement reliability. In total, 216 prepared and milled coal samples were analyzed using this setup, and for each individual sample, the complete particle size distribution profile was recorded. Subsequently, the five most widely used characteristic size parameters—namely D10, D50, D90, D32 (Sauter mean diameter), and D43 (De Brouckere mean diameter) were extracted from the cumulative distribution curves, along with the specific surface area, i.e. SSA were determined. These parameters were selected to comprehensively characterize both the fine and coarse fractions of the particle population as well as the surface- and volume-weighted particle size characteristics.

The specific surface area (SSA) of the same prepared and grinded coal samples was also determined to quantify the total surface available for oxygen adsorption and coal–oxygen interactions. Since spontaneous combustion is initiated by surface oxidation reactions, SSA provides a critical measure of the reactive surface exposed to atmospheric oxygen. Consequently, the combined use of PSD and SSA measurements enabled a detailed characterization of the physical factors governing coal oxidation kinetics and self-heating behavior. Explanation for the size parameters and corresponding mathematical equations (Eqn.1 and Eqn.2) are provided as in the following:

D_{10} (μm): sieve opening which 10 % of particles passing through

D_{50} (μm): sieve opening which 50 % of particles passing through

D_{90} (μm): sieve opening which 90 % of particles passing through

D_{32} (μm): volume / surface mean (Sauter Mean)

Sauter mean is defined as the diameter of a sphere that has the same volume/surface ratio as a particle of interest.

$$D_{32} = \frac{\sum_1^n {D_i}^3 \nu_i}{\sum_1^n {D_i}^2 \nu_i} \quad (1)$$

D_{43} (μm): the mean diameter over volume (DeBrouckere Mean)

$$D_{43} = \frac{\sum_1^n {D_i}^4 \nu_i}{\sum_1^n {D_i}^3 \nu_i} \quad (2)$$

The obtained PSD and SSA data were subsequently correlated with the spontaneous combustion liability indices, namely the Feng–Chakravorty–Cochrane (FCC), Crossing Point Temperature (CPT), and Average Temperature Increase (ATI), to evaluate the extent to which particle size characteristics and surface area influence coal oxidation reactivity and spontaneous combustion propensity.

2.2.2. Coal Spontaneous Combustion Liability Tests

Coal spontaneous combustion liability was assessed using the Crossing Point Temperature (CPT) method, which is widely accepted as one of the most reliable indicators of a coal's self-heating propensity. The CPT corresponds to the temperature at which the heat generated by coal oxidation surpasses the rate of heat dissipation, causing the coal temperature to increase more rapidly than the surrounding environment. Owing to its direct relationship with oxidation reactivity, CPT has been extensively employed to evaluate spontaneous combustion susceptibility across a broad range of coal types.

In addition to CPT, the spontaneous combustion characteristics of the coal samples were quantified using the Feng–Chakravorty–Cochrane (FCC) Index, originally proposed by Feng et al. (1973). The experimental system consisted of a reaction vessel housed within a temperature-controlled furnace, together with an air supply unit, thermocouple sensors, and temperature monitoring equipment. The setup can also be coupled with an online gas chromatograph to monitor gaseous oxidation products generated during the experiment (Figure 4).

Prior to testing, the coal samples were pulverized to a particle size finer than 200 mesh. Representative subsamples weighing 35 g were prepared, with one additional sample retained as a duplicate. Each sample was placed in the reactor and subjected to a programmed heating regime. The furnace temperature was initially stabilized at ambient conditions and subsequently increased at a constant heating rate of 0.5 °C min^{-1} until a temperature exceeding 220 °C was reached. Once thermal equilibrium between the furnace and the coal sample had been established, air was introduced at a flow rate of 100 mL min^{-1} to initiate the oxidation process. The temperature at which the coal sample temperature intersected and exceeded the furnace temperature was recorded as the CPT value. Furthermore, the average temperature increase observed between 110 and 220 °C was calculated and subsequently used to determine the FCC Index according to Eqn.3 (Bilen et al., 2026).

$$FCC\ Index\ =\ 1000x\frac{average\ teperature\ increase\ between\ 110-220\ °C}{crossing\ point\ temperature\ °C} \quad (3)$$

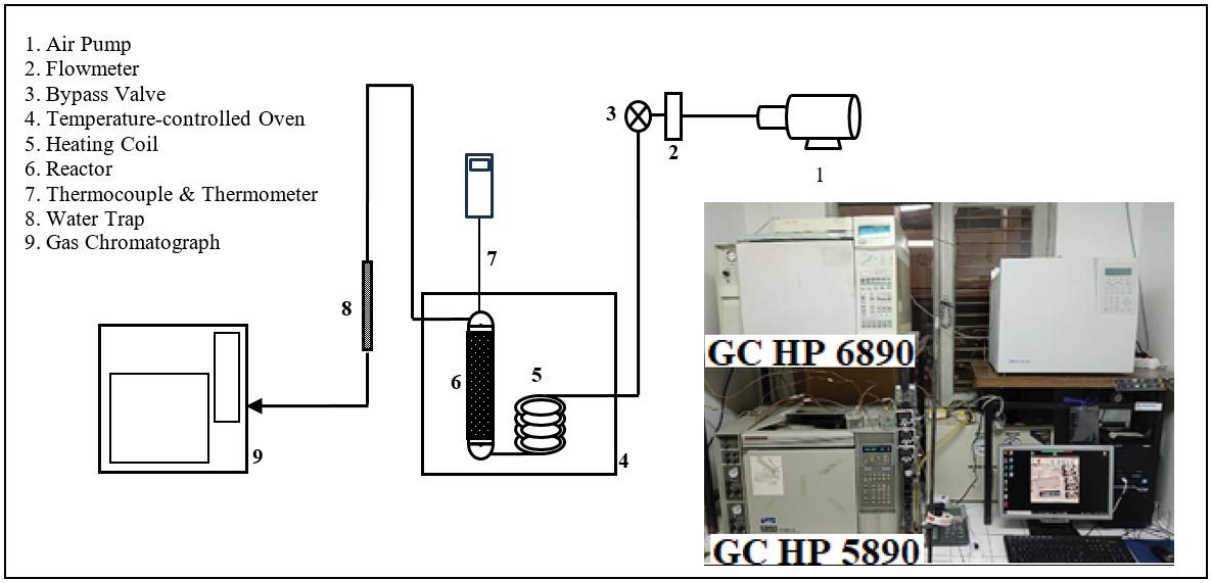


Figure 4. Schematic representation of the experimental apparatus employed for the CSC liability measurements (Bilen 2025, Bilen et al., (2026)).

The risk classification based on FCC Index values suggested by Feng et al. (1973) is given in Table 1 (Bilen et al. 2026).

Table 1. Risk classification in terms of FCC index.

FCC Index	Risk Classification
0 - 5	Low
5 -10	Middle
> 10	High

3. Results and Discussion

The complete dataset obtained from the experimental investigations is presented in Appendix Table A1, which contains the results of all 216 coal samples analyzed in this study. The appendix includes the detailed particle size distribution (PSD) descriptors, namely D10, D50, D90, D32, and D43, together with specific surface area (SSA) values and the corresponding

436 spontaneous combustion liability indices, including Crossing Point Temperature (CPT),
437 Average Temperature Increase (ATI), and the Feng–Chakravorty–Cochrane (FCC) Index.
438
439 Considering the large number of samples and the broad variability among coal types, an initial
440 descriptive statistical evaluation was conducted to establish the overall distribution
441 characteristics of the investigated variables. Accordingly, the minimum, maximum, and
442 average values of the PSD parameters, SSA, and spontaneous combustion indices were
443 calculated and are summarized in Table 2.
444
445 Table 2. Descriptive statistics of PSD parameters, SSA, and spontaneous combustion liability
446 indices (n = 216).

Parameter	Minimum	Maximum	Average
D10 (μm)	0.47	80.79	3.68
D50 (μm)	3.48	75.87	31.26
D90 (μm)	8.19	271.17	96.74
D32 (μm)	1.36	6.51	4.55
D43 (μm)	4.03	110.45	41.99
SSA (m^2/g)	0.92	4.42	1.46
CPT (°C)	134.00	205.00	162.94
ATI (°C/min)	0.49	2.39	0.91
FCC	2.48	13.87	5.69

447
448 The descriptive statistics demonstrate a remarkably broad variability among the investigated
449 coal samples, indicating substantial heterogeneity in particle-scale characteristics and

spontaneous combustion behavior. Such variability provides a suitable basis for evaluating the influence of PSD and SSA on coal oxidation liability across different coal ranks and geological origins. Illustration of the relationships between D10, D50, D90, D32, D43 and SSA with respect to CPT values is provided in Figure 5. Likewise the representation of the relationships between D10, D50, D90, D32, D43 and SSA with respect to ATI values is provided in Figure 6. Last but not the least, graphical demonstration of the relationships between D10, D50, D90, D32, D43 and SSA with respect to FCC values is provided in Figure 7.

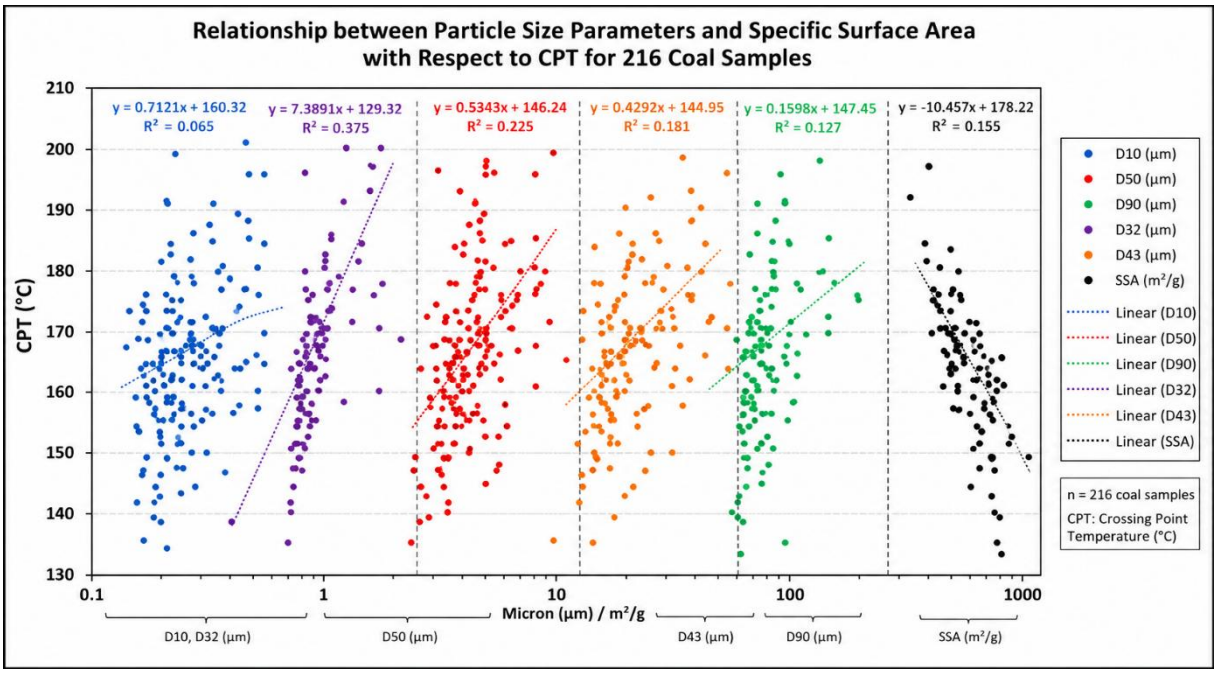
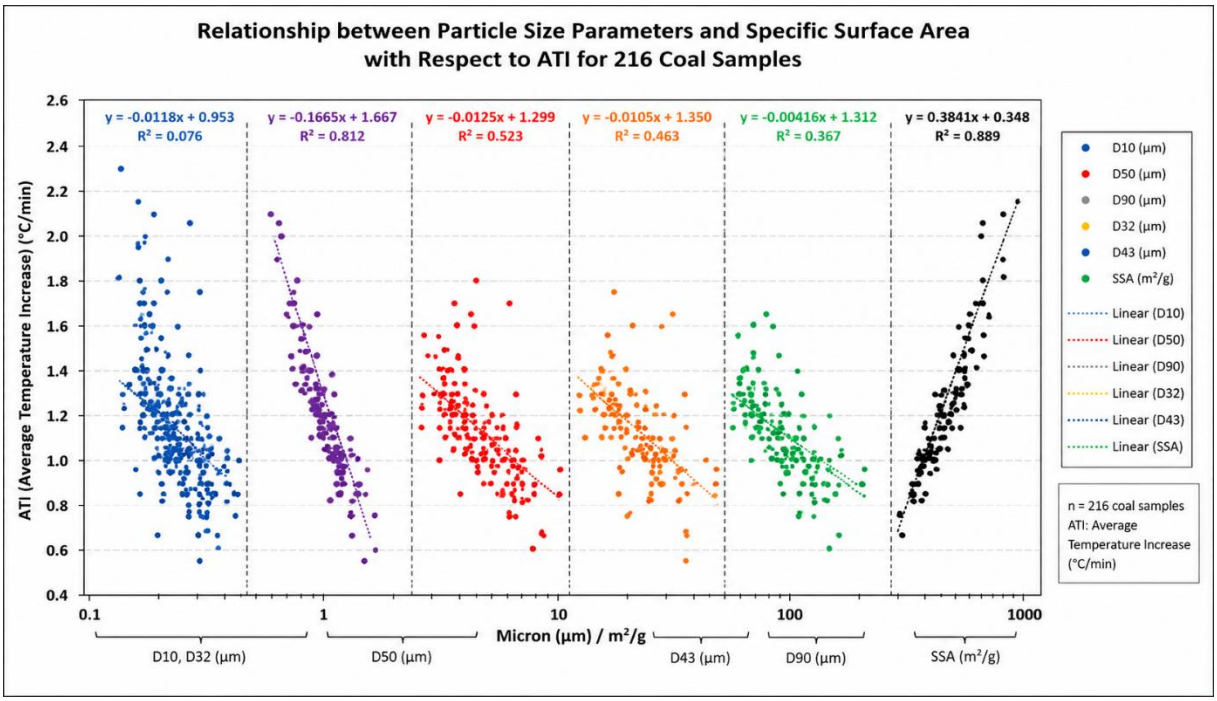


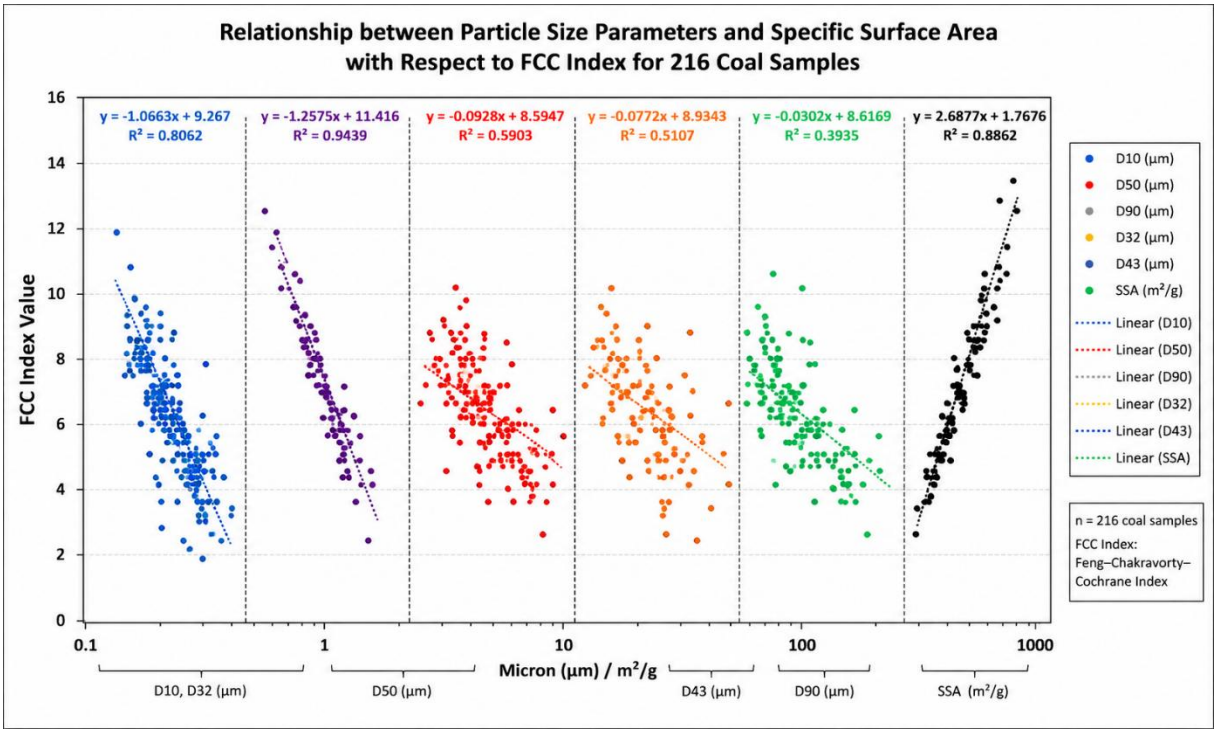
Figure 5. Relationships between D10, D50, D90, D32, D43 and SSA with respect to CPT values



461

462 Figure 6. Relationships between D10, D50, D90, D32, D43 and SSA with respect to ATI values

463



464

465 Figure 7. Relationships between D10, D50, D90, D32, D43 and SSA with respect to FCC values

466

The results indicate that decreasing D10 values generally correspond to lower CPT values and higher ATI and FCC values. Since D10 represents the finest 10% fraction of the particle population, reductions in D10 imply an increased abundance of ultrafine particles, thereby increasing the reactive surface available for oxygen adsorption. Consequently, oxidation reactions accelerate, leading to enhanced spontaneous combustion susceptibility.

Among all PSD descriptors, D50 exhibited one of the strongest relationships with spontaneous combustion behavior. Coal samples characterized by smaller median particle diameters consistently demonstrated lower thermal stability and increased oxidation reactivity. This observation suggests that median particle size is an important indicator governing heat accumulation processes.

D90 represents the coarse particle fraction. As D90 decreased, ATI and FCC values generally increased, while CPT values tended to decrease. This behavior indicates that even the coarser particle population contributes significantly to overall oxidation behavior by influencing particle packing density and oxygen accessibility.

D32 emerged as one of the most influential PSD descriptors throughout the entire dataset. Since D32 represents the Sauter mean diameter and directly incorporates the surface-to-volume relationship, its physical significance is strongly associated with oxygen accessibility and oxidation kinetics. Indeed, D32 exhibited exceptionally strong relationships with ATI and FCC values, indicating that this parameter may serve as one of the most reliable predictors of spontaneous combustion liability.

Furthermore, the D43 parameter, representing the volume-weighted mean particle diameter and placing greater emphasis on the contribution of coarse particles, also exhibited discernible relationships with the spontaneous combustion characteristics of the investigated coal samples. Although statistically significant correlations were obtained, the strength of these relationships was comparatively lower than those associated with the D32 parameter. This observation suggests that particle size descriptors dominated by volumetric contributions alone are not sufficient to fully explain the self-heating behavior of coal. Instead, parameters reflecting the balance between particle size and available surface area appear to play a more critical role in determining oxidation susceptibility. In particular, D32, which is directly associated with the volume-to-surface area ratio of particles, demonstrated superior sensitivity toward changes in spontaneous combustion indices, highlighting the dominant influence of surface-related phenomena during the early stages of coal oxidation. Consequently, while D43 remains a useful indicator for describing the overall coarseness of the particle population, the results indicate that surface-controlled mechanisms exert a considerably stronger influence on spontaneous combustion propensity than purely volume-based characteristics.

Similarly, the effect of specific surface area (SSA) on spontaneous combustion liability was found to be highly pronounced and consistent throughout the experimental investigation. Coal samples characterized by elevated SSA values invariably exhibited lower Crossing Point Temperature (CPT) values together with substantially higher Average Temperature Increase (ATI) and FCC values, indicating enhanced oxidation activity and a greater tendency toward self-heating. Such behavior can be attributed to the fact that an increase in specific surface area provides a larger number of reactive sites available for oxygen adsorption, thereby promoting oxygen diffusion and accelerating exothermic oxidation reactions. As a consequence, the thermal stability of coal particles decreases with increasing surface area, making finely divided

materials considerably more susceptible to spontaneous combustion. A comprehensive evaluation of all particle size distribution parameters and combustion indices further reveals that spontaneous combustion liability is governed by the combined effects of particle size reduction and the corresponding enhancement of surface area. In general, finer particles exhibited greater oxidation reactivity, lower thermal resistance, and more pronounced self-heating characteristics. Although each PSD parameter contributed to the observed behavior to varying extents, the findings clearly demonstrate that D32 and SSA emerged as the most sensitive and reliable indicators for assessing spontaneous combustion propensity, emphasizing the predominant role of surface-related properties in controlling the oxidation kinetics and thermal behavior of coal particles.

These findings clearly indicate that surface-controlled oxidation mechanisms dominate the spontaneous combustion process. The findings obtained in this study are highly consistent with previously published experimental investigations. Firstly, the observed increase in spontaneous combustion liability with decreasing particle size strongly supports the pioneering studies conducted by Jia et al. (2022), Zhang et al. (2011), and Yu et al. (2016), who demonstrated that finer particles exhibit higher oxygen adsorption capacities and accelerated oxidation kinetics. The present study extends these earlier observations by systematically quantifying this relationship through multiple PSD descriptors rather than isolated particle size classes. In addition, Qin et al. (2010) reported that coal fractions below 0.9 mm exhibit substantially higher oxidation rates than coarser particles. The present results strongly corroborate these findings, as lower D10, D50, and D90 values consistently corresponded to increased FCC and ATI values.

The present results also agree remarkably well with Yang et al. (2019), who demonstrated that particle size not only influences macroscopic oxidation behavior but also alters the evolution of free radicals and oxygen-containing functional groups. Although molecular analyses were beyond the scope of the present study, the strong dependency observed between PSD descriptors and combustion indices indirectly supports the underlying chemical mechanisms proposed by these authors.

Moreover, the exceptionally strong influence of SSA observed herein is highly consistent with the findings of Mishra (2022) and Mishra et al. (2025). Their studies emphasized that specific surface area is one of the primary governing factors controlling oxygen adsorption, heat generation, and self-heating propensity. The present investigation further strengthens this conclusion by demonstrating that SSA exhibits one of the strongest relationships with ATI and FCC across an extensive dataset of 216 samples.

Additionally, Wang et al. (2016) suggested the existence of threshold behavior at very fine particle sizes, where oxidation rates eventually approach saturation. Although the present study did not explicitly investigate threshold phenomena, the slight dispersion observed within the ultrafine particle domain may indirectly support this hypothesis.

Similarly, Zhang et al. (2014) emphasized the synergistic interactions among particle size, porosity, and surface area during heat accumulation processes. The current findings strongly reinforce this interpretation, indicating that PSD descriptors alone cannot fully explain spontaneous combustion behavior unless considered together with SSA.

Overall, the present study substantially advances existing knowledge by integrating six particle-scale descriptors with three established spontaneous combustion liability indices within a single comprehensive framework. Unlike previous studies, which primarily focused on isolated particle size fractions or individual oxidation indicators, this research demonstrates that PSD and SSA collectively provide a robust multi-parameter approach for spontaneous combustion prediction.

Consequently, these findings offer significant practical implications for mine fire prevention strategies, early warning systems, and risk assessment protocols, particularly in environments where heterogeneous coal particle mixtures are continuously generated during mining, transportation, crushing, and handling operations.

4. Conclusion

This study comprehensively evaluated the influence of particle size distribution (PSD) and specific surface area (SSA) on coal spontaneous combustion (CSC) liability using an extensive dataset consisting of 216 coal samples with diverse physicochemical properties and geological origins. By integrating multiple PSD descriptors (D10, D50, D90, D32, and D43) with three established spontaneous combustion liability indices, namely Crossing Point Temperature (CPT), Average Temperature Increase (ATI), and the Feng–Chakravorty–Cochrane (FCC) Index, a multidimensional framework was established to better understand the role of particle-scale characteristics in governing coal oxidation behavior. The findings clearly demonstrate that spontaneous combustion susceptibility is strongly controlled by the interaction between particle size reduction and surface area enhancement, both of which directly influence oxygen accessibility and oxidation kinetics.

The results further indicate that spontaneous combustion behavior cannot be adequately explained by a single particle size parameter alone. Instead, it is governed by a combination of surface-related and volumetric particle characteristics acting simultaneously. Among all investigated variables, D32 and SSA emerged as the most sensitive indicators of oxidation propensity, emphasizing the dominant role of surface-controlled mechanisms throughout the self-heating process. Overall, this study provides a more comprehensive understanding of coal spontaneous combustion behavior and demonstrates that integrating PSD descriptors with SSA measurements can significantly improve spontaneous combustion assessment methodologies and enhance practical risk evaluation strategies used in mining operations.

The principal findings of this study can be summarized as follows:

- Decreasing particle size consistently increased spontaneous combustion liability, as evidenced by lower CPT values and higher ATI and FCC values, indicating enhanced oxidation reactivity and stronger self-heating tendencies.
- D32 was identified as one of the most influential PSD descriptors, suggesting that parameters incorporating the surface-to-volume relationship are particularly effective for evaluating spontaneous combustion susceptibility.
- Specific surface area (SSA) exhibited a pronounced influence on oxidation behavior, confirming that oxygen-accessible reactive surfaces play a critical role in governing coal self-heating processes.
- The combined use of PSD descriptors and SSA provided a more robust and representative assessment framework than approaches based solely on individual particle size fractions, thereby offering improved potential for spontaneous combustion prediction and risk classification.

Future studies should focus on expanding the proposed framework by integrating PSD and SSA measurements with advanced physicochemical characterization techniques, including pore structure analysis, gas evolution monitoring, free radical determination, and functional group transformations during oxidation. In addition, incorporating environmental variables such as moisture content, oxygen concentration, airflow conditions, and ambient temperature into predictive models may further improve the understanding of spontaneous combustion mechanisms. The integration of these parameters with data-driven approaches, particularly machine learning and artificial intelligence techniques, may ultimately facilitate the development of intelligent real-time monitoring and early warning systems for safer and more sustainable mining operations.

Author contribution statement

Yilmaz, S: Conceptualization, Resources, Validation, Visualization, Writing – original draft, Writing – Review and Editing, Supervision, Project Administration

Bilen, M: Methodology, Formal Analysis, Investigation, Data Curation, Resources, Validation

Barış, K: Conceptualization, Supervision, Writing – Original Draft, Writing – Review & Editing, Project Administration.

Funding statement

No funding was received.

Data availability statement

The corresponding data included in the context of this paper is available upon request.

Declaration of competing interest

No potential competing interest was reported by the authors.

Acknowledgements

The authors gratefully acknowledge the support provided by Zonguldak Bülent Ecevit University Scientific Research Projects Coordination Unit (BAP) under Project No. 2025-29011448-01. This support was instrumental in the successful completion of the experimental and analytical components of this study. The authors would also like to express their sincere appreciation to Mr. Yasin Ramish, M.Sc. student, for his valuable assistance in conducting the coal spontaneous combustion experiments. In addition, special thanks are extended to Dr. Emre Günay, Postdoctoral Researcher, for his significant contributions to the experimental work and technical support throughout the study.

651 **TABLE A1.** Complete dataset of 216 coal samples.

No	Sample	Moisture % (a.r.)	Ash % (a.r.)	Volatile Matter % (a.r.)	Fixed Carbon % (a.r.)	Sulfur % (a.r.)	D10	D50	D90	D32	D43	SSA	CPT	ATI	FCC
1	Afyon Sincanlı	41.70	8.29	22.56	27.45	3.06	1.75	22.98	90.25	3.18	35.94	1.8841	197.00	1.38	6.99
2	Çayırhan 1	18.36	30.04	28.09	23.51	2.87	1.02	8.92	71.91	2.16	24.39	2.7788	167.50	1.52	9.10
3	Çayırhan 2	25.78	14.28	32.11	27.83	2.98	1.78	14.74	53.75	2.89	22.58	2.0772	181.50	1.35	7.41
4	Amasya Beşler	10.93	12.02	35.97	41.08	0.85	1.1	12.89	60.15	2.23	23.04	2.696	158.50	1.33	8.40
5	Amasya Plt	10.50	38.04	27.80	23.66	0.72	2.79	26.13	77.05	3.89	34	1.5409	141.50	0.89	6.28
6	Amasya Yeni Anadolu	7.60	59.42	17.59	15.39	0.20	4.63	34.9	107.37	5.74	47.28	1.0454	158.50	0.69	4.33
7	Aydın Atay	13.98	20.39	36.09	29.54	1.49	2.78	23.59	71.96	3.87	31.32	1.5489	157.50	1.00	6.32
8	Aydın Yeni Volkan	15.72	5.36	40.29	38.63	1.95	1.74	11.91	43.43	2.74	18.36	2.1901	153.50	1.15	7.48
9	Aydın Bükköy	12.10	17.10	37.03	33.77	1.54	4.01	34.44	90.17	5.12	41.5	1.1727	150.50	0.78	5.16
10	Amasra1	1.30	14.49	32.14	52.07	0.60	2.86	41.17	136.65	4.73	56.93	1.2689	145.00	0.84	5.79
11	Amasra2	1.30	23.92	32.87	41.91	0.60	3.68	34.21	87.34	4.87	40.58	1.2309	145.00	0.80	5.51
12	Yılmaz 1	26.60	8.35	29.43	35.62	1.12	0.47	3.75	10.61	1.37	5.85	4.3954	173.00	1.84	10.65
13	Yılmaz 2	23.70	14.41	29.51	32.38	1.14	1.77	20.44	94.98	3.02	36.43	1.9838	168.50	1.23	7.28
14	Yılmaz 3	24.40	17.03	27.14	31.43	1.11	2.72	21.59	73.11	3.97	31.45	1.5095	168.00	1.04	6.21
15	Yılmaz 4	26.60	7.16	32.32	33.92	1.11	2.01	16.82	56.9	3.17	24.29	1.8953	179.00	1.26	7.01
16	Kütahya Park	8.80	25.33	29.11	36.76	0.78	3.44	30.51	80.93	4.89	37.23	1.2262	147.00	0.80	5.46
17	Kütahya Gediz	1.84	27.85	28.14	42.17	6.63	4.42	30	92.17	5.35	40.45	1.1213	166.00	0.80	4.85
18	Kütahya Atıl-Al	13.10	12.12	32.05	42.73	6.68	2.15	24.66	149.18	3.39	50.52	1.7684	160.00	1.10	6.88
19	Fernas 1	12.60	5.17	37.01	45.22	1.24	4.14	37.06	104.71	5.19	46.75	1.156	160.50	0.81	5.04
20	Fernas 2	15.00	7.89	35.22	41.90	1.20	3.79	23.72	77.53	4.85	33.83	1.238	159.00	0.89	5.61
21	İmbat1	10.60	20.89	32.70	35.80	0.99	3.18	49.19	115.9	5.09	54.42	1.1785	156.50	0.82	5.21
22	İmbat2	12.00	29.43	28.96	29.61	0.98	4.4	43.23	118.72	6.06	53.73	0.9903	168.50	0.65	3.85

23	Armutçuk1	0.90	6.28	34.94	57.88	0.52	3.88	26.74	107.31	4.61	43.01	1.3019	155.00	0.90	5.81
24	Armutçuk2	0.92	6.45	34.87	57.76	0.52	2.64	26.71	77.26	4.33	34.43	1.3856	151.00	0.90	5.97
25	Gelik1	2.20	29.32	23.61	44.97	0.61	3.91	34.98	102.29	5.25	45.41	1.1434	178.50	0.88	4.93
26	Gelik2	1.70	46.08	17.78	34.44	0.33	5.23	34.74	102.99	6.38	45.95	0.9399	199.00	0.63	3.16
27	Karadon1	2.20	25.19	24.86	47.75	0.53	4.76	41.72	105.67	6.44	49.5	0.9323	201.00	0.62	3.07
28	Karadon2	2.10	29.32	23.61	44.97	0.51	4.51	54.67	152.65	6.39	67.96	0.9384	200.00	0.63	3.16
29	Kozlu1	1.30	15.56	27.26	55.88	0.50	4.4	28.04	77.07	5.63	35.67	1.0666	175.50	0.78	4.46
30	Kozlu2	2.20	7.32	29.55	60.93	0.48	4.26	27.02	84.95	5.29	37.12	1.1334	166.50	0.82	4.90
31	Üzülmez1	1.10	10.19	27.94	60.77	0.57	4.47	38.29	116.13	5.75	50.62	1.0428	179.50	0.77	4.30
32	Üzülmez2	1.30	8.19	29.47	61.04	0.56	3.94	42.3	106.85	5.67	49.72	1.059	177.50	0.79	4.45
33	Bursa Bükköy	13.57	12.67	38.82	34.94	3.27	2.77	20.61	71.06	3.88	30.09	1.5458	150.50	0.95	6.29
34	Çan 1	16.08	7.74	37.83	38.35	2.01	3.42	38.81	112.46	5.01	49.55	1.1978	154.00	0.81	5.25
35	Çan 2	14.50	15.71	33.43	36.36	2.06	4.25	28.17	79.34	5.46	36.39	1.0983	150.00	0.70	4.67
36	Bolu Mengen 1	9.00	10.18	42.75	38.07	8.20	1.53	16.81	76.53	2.68	29.52	2.2419	145.50	1.11	7.61
37	Bolu Mengen 2	8.82	8.32	39.59	43.27	8.22	0.9	11.16	93.25	2.09	32.44	2.8682	144.50	1.32	9.15
38	Bolu Mengen 3	6.24	7.08	46.18	40.50	8.67	2.09	20.53	84.28	3.36	33.36	1.7867	152.50	1.06	6.96
39	Bartın Hattat	3.58	13.62	33.42	49.38	1.08	1.42	12.74	52.58	2.45	20.88	2.4449	135.00	1.09	8.08
40	Eskişehir Adularya	29.64	30.16	21.40	18.80	1.41	3.45	33.73	110.2	5.16	46.64	1.1626	169.50	0.86	5.06
41	Artvin Yusufeli No:3	4.64	22.84	22.50	50.02	2.74	4.62	35.19	100.15	5.49	45.21	1.0931	171.00	0.79	4.60
42	Artvin Yusufeli No:4	2.38	25.16	22.71	49.75	2.78	4.2	34.22	101.62	5.2	44.73	1.154	163.00	0.82	5.04
43	Artvin Yusufeli No:5	1.24	32.30	21.51	44.95	2.63	4.49	38.06	92.68	6.12	44.17	0.9812	180.00	0.67	3.72
44	defaş 1 km2	16.74	12.84	33.16	37.26	0.99	3.72	23.88	80.98	4.83	34.87	1.241	157.00	0.89	5.65
45	demir export m3	11.44	15.48	36.28	36.80	1.06	1.42	15.04	66.9	2.52	26.01	2.3769	147.00	1.18	8.00
46	demir export ayak	11.30	23.78	32.83	32.09	1.00	1.36	10.57	43.07	2.53	17.85	2.3683	145.00	1.16	7.98
47	erz şenkaya taban	7.08	33.49	26.90	32.53	0.98	1.49	18.81	77.59	2.63	30.5	2.2852	142.00	1.12	7.90
48	erz şenkaya tavan	6.99	7.74	36.16	49.11	1.14	2.46	16.62	56.59	3.58	24.49	1.6759	134.00	0.89	6.66

49	imbat km2	12.68	5.54	36.98	44.80	0.92	1.4	12.93	54.33	2.33	21.41	2.5759	147.00	1.23	8.36
50	Nevşehir Gülşehir	8.72	29.97	28.38	32.93	5.50	2.8	23.43	92.3	3.9	37.03	1.5399	144.00	0.90	6.28
51	Edirne Üçel 4	15.84	28.77	30.13	25.26	1.97	3.7	25.43	70.69	4.96	32.38	1.2088	156.50	0.84	5.39
52	Edirne Özşen 4	14.72	54.36	22.42	8.50	0.32	4.41	32.64	98.77	5.38	43.33	1.116	160.50	0.77	4.82
53	Edirne Üçel 1	15.90	32.29	28.12	23.69	0.82	3.12	21.35	69.65	4.22	30.32	1.4202	151.50	0.92	6.06
54	Edirne Keşan 1	15.20	21.14	33.59	30.07	3.51	1.72	11.21	58.61	2.69	22.17	2.2319	158.50	1.19	7.49
55	Malkara Global 1	35.34	6.67	28.50	29.49	0.61	0.47	3.48	8.19	1.36	4.03	4.4213	172.00	2.39	13.87
56	Sorgun 2	7.76	32.06	31.73	28.45	8.43	3.04	43.1	144.28	4.38	59.79	1.3689	145.50	0.86	5.89
57	Malkara Kar-Deniz 1	19.42	38.75	26.11	15.72	0.68	2.43	34.04	93.14	3.97	41.62	1.5118	167.50	1.05	6.25
58	Mengen 2	10.56	8.26	47.10	34.08	9.07	2.15	27.12	118.42	3.62	45.85	1.6592	153.50	0.99	6.47
59	Milas 2	26.22	11.44	36.37	25.97	5.21	0.74	7.53	47.11	1.76	17.88	3.418	163.50	1.67	10.20
60	Mugla Aydın 1	25.76	8.03	38.18	28.03	4.96	1.57	22.28	99.22	2.94	38.22	2.038	171.50	1.27	7.39
61	Denizli Alt	27.68	17.98	35.52	18.82	1.44	1.26	10.85	46.09	2.47	18.7	2.4309	174.50	1.40	8.03
62	Denizli Üst	27.80	17.61	35.07	19.52	1.70	2.2	17.6	60.29	3.43	25.88	1.7498	176.50	1.21	6.85
63	Zonguldak Sfh Çay	1.25	7.34	30.02	61.39	0.28	1.31	9.83	39.81	2.41	16.41	2.4888	144.50	1.17	8.10
64	Zonguldak Ofkar	1.80	8.32	37.46	52.42	0.83	1.53	12.75	50.18	2.56	20.26	2.3403	141.50	1.13	7.96
65	Zonguldak Demir	1.20	7.52	32.32	58.96	0.41	2.46	16.83	47.7	3.51	21.63	1.7074	147.50	1.00	6.76
66	Zonguldak Yıldız	1.84	14.64	33.90	49.62	0.76	1.93	18.3	66.46	3.01	27.29	1.9928	143.50	1.05	7.34
67	Zonguldak Sfh Akalın	1.25	4.37	29.92	64.45	0.40	2.8	31.01	121.45	4.33	48.37	1.3867	149.50	0.90	5.99
68	Kütahya Bozdağ B5	7.40	19.62	34.62	38.36	2.84	3.6	35.72	102.71	4.98	45.65	1.204	148.00	0.78	5.26
69	Kütahya Altıntaş Tek	7.44	31.50	35.70	25.36	3.77	4.94	39.4	105.52	6.25	48.3	0.9594	173.00	0.61	3.52
70	Kütahya Bozdağ Tv. B5	7.30	31.74	32.10	28.86	2.25	3.8	28.51	84.34	5.01	37.25	1.1977	148.00	0.78	5.25
71	Kütahya Altıntaş 3	7.22	26.78	34.91	31.09	4.69	3.42	31.92	99.76	4.76	43.23	1.2593	152.00	0.87	5.72
72	Ermenek Üçpınar	31.40	11.30	33.32	23.98	3.31	2.68	19.29	65.68	3.62	27.98	1.6579	165.00	1.06	6.44
73	Mengen 1	6.80	5.25	52.36	35.59	8.74	3.12	22.54	70.14	4.16	30.75	1.443	150.00	0.91	6.09
74	Ermenek Seba	18.54	20.25	37.64	23.57	4.25	2.4	19.34	56.13	3.62	26.09	1.6555	165.00	1.06	6.44

75	Milas Kinetik	25.00	11.09	36.69	27.22	5.22	0.64	7.36	44.17	1.68	16.09	3.5643	168.50	1.76	10.47
76	Soma Y.A. 1	15.60	23.81	34.59	26.00	4.28	1.46	13.17	103.93	2.66	35.29	2.2564	143.50	1.12	7.81
77	Tire Kot A	26.75	6.39	37.69	29.17	1.83	3.75	33.37	107.87	4.98	46.48	1.2043	171.50	0.92	5.36
78	Tire Kot B	27.74	6.51	35.28	30.46	1.61	2.35	21.03	67.24	3.49	29.11	1.7185	172.50	1.17	6.78
79	Soma İmbat KM-2_1	4.41	12.58	39.35	43.67	1.12	1.27	11.74	54.66	2.2	20.99	2.7261	146.50	1.24	8.47
80	Kınık Polyak	12.18	27.78	36.79	23.25	2.10	3.14	23.68	69.59	4.23	31.29	1.4195	144.50	0.88	6.06
81	Soma İmbat KM-2_2	12.40	15.69	34.89	37.02	1.08	1.82	17.92	81.09	3.06	31.56	1.9577	145.50	1.05	7.23
82	Tire Kot C	26.80	13.04	32.94	27.22	3.49	2.03	26.01	101.47	3.58	40.42	1.6741	146.50	0.97	6.63
83	Kınık CK1109	11.46	20.20	38.88	29.46	2.16	5.07	38.89	109.33	5.98	49.56	1.0029	170.50	0.69	4.05
84	Tosya Öngür 80	13.54	39.23	32.05	15.18	6.37	1.14	13.65	89.93	2.39	31.95	2.5063	140.50	1.17	8.31
85	Zonguldak Ofkar 1	1.69	6.49	38.74	53.08	0.76	2.28	32.63	105.83	3.74	44.84	1.6023	151.50	0.97	6.40
86	Edirne Şenbaş	15.98	18.05	34.57	31.40	0.63	2.23	21.15	94.4	3.41	36.37	1.759	142.50	0.98	6.88
87	Zonguldak Yıldız 2	1.63	9.59	39.02	49.76	2.44	2.3	16.88	50.57	3.62	23.54	1.6593	161.50	1.06	6.55
88	Dodurga Taban	24.20	23.50	27.65	24.65	0.94	3.5	33.38	108.71	4.89	46.16	1.2276	166.50	0.91	5.48
89	Tosya Öngür 120	18.08	14.83	35.43	31.66	6.43	2.37	17.24	60.65	3.46	25.65	1.7333	159.50	1.09	6.85
90	Dodurga Tavan	25.00	4.71	32.87	37.42	1.81	5.05	38.63	122.85	5.85	53.05	1.0265	164.50	0.70	4.25
91	Edirne Özşen 4P	15.58	57.62	19.64	7.16	1.14	3.61	42.44	118.33	5.19	52.58	1.1564	169.50	0.86	5.06
92	Zonguldak Derinsu	1.30	4.80	29.94	63.96	0.39	2.78	23.8	78.59	3.84	33.36	1.5631	151.50	0.96	6.35
93	Akkurt Acılık	2.05	3.94	30.61	63.40	0.39	2.67	22.12	70.01	3.84	30.13	1.5606	151.50	0.96	6.35
94	Akkurt Hacımemiş	2.12	6.12	29.56	62.20	0.70	0.88	10.2	46.37	1.88	17.77	3.1992	141.00	1.38	9.78
95	Entegre Domuzcu	1.38	8.49	32.26	57.87	0.41	2.8	35.83	95.64	4.42	43.32	1.3581	152.50	0.89	5.85
96	Entegre Seksenlik	1.84	10.71	30.96	56.49	0.76	2.59	16.97	63.42	3.56	26.1	1.6858	167.00	1.12	6.69
97	Malatya Bahadır 1	18.72	25.14	31.85	24.29	0.92	2.61	33.56	101.62	3.95	43.71	1.5184	167.50	1.05	6.27
98	Malatya Bahadır 2	18.71	23.69	32.24	25.36	0.92	2.94	49.7	117.68	4.84	55.19	1.2409	145.50	0.82	5.64
99	Gümüşhane Başkan 1	4.92	38.75	27.42	28.91	0.87	3.13	42.35	112.77	4.44	50.97	1.3502	147.50	0.86	5.85
100	Gümüşhane Başkan 2	4.00	38.41	28.42	29.17	0.88	2.45	21.1	69.75	3.65	29.89	1.6452	143.50	0.92	6.44

101	Gümüşhane Başkan 3	3.92	58.47	22.32	15.29	0.22	2.01	24.84	97.09	3.55	38.75	1.6918	134.50	0.90	6.70
102	ZS1N1	2.20	50.10	21.50	26.20	0.70	3.22	37.74	99.34	4.95	45.36	1.2127	160	0.82	5.42
103	ZS1N2	2.20	54.20	18.50	25.10	0.80	2.9	63.95	171.79	4.85	76.03	1.2368	162.5	0.85	5.6
104	ZS1N3	2.80	44.20	20.60	32.40	0.70	3.23	41.8	113.61	5.12	51.03	1.171	158	0.79	5.1
105	ZS1N4	4.40	16.30	25.60	53.60	0.80	4.98	37.23	104.71	6.01	47.38	0.9986	170	0.7	4
106	ZS1N5	6.40	26.10	24.20	43.30	0.80	4.77	32.66	87.68	5.68	40.61	1.0561	168.5	0.74	4.35
107	ZS1N6	10.20	42.80	16.10	30.90	1.00	2.88	20.06	60.55	4.09	27.06	1.4655	152	0.95	6.1
108	ZS2N02-1	3.37	18.53	27.59	50.51	0.52	3.49	34.71	92.21	5.43	42.6	1.1047	165	0.78	4.75
109	ZS2N02-2	4.23	30.09	21.75	43.93	0.40	3.96	46.57	124.63	5.77	56.34	1.0394	162	0.73	4.3
110	ZS2N03	7.11	24.75	23.79	44.35	0.40	3.52	46.24	124.91	5.51	56.29	1.0898	160.5	0.76	4.55
111	ZS2N04	10.64	55.34	14.57	19.44	0.52	2.29	17.03	52.7	3.49	23.94	1.7188	150	1.02	6.85
112	ZS2N05	5.29	13.10	28.47	53.14	0.50	4.23	56.55	172.37	6.05	73.56	0.9919	172	0.69	3.95
113	ZS2N06	10.73	23.36	22.92	42.99	0.40	3.94	29.22	97.54	5.3	41.92	1.1326	164	0.81	4.9
114	ZS2N07	6.88	16.10	25.00	52.02	0.46	3.46	58.6	122.76	5.68	61.46	1.0569	168	0.74	4.4
115	ZS3N01	10.12	18.53	24.71	46.64	0.44	3.31	43.47	98.87	5.15	47.83	1.166	165.5	0.83	5.1
116	ZS3N02	1.94	64.19	15.64	18.23	0.35	4.9	37.99	107.93	6.2	48.2	0.9677	170	0.67	3.6
117	ZS3N03	2.95	59.68	16.07	21.30	0.52	3.36	21.47	70.38	4.45	30.81	1.3498	158.5	0.88	5.85
118	ZS3N04	9.42	33.77	20.70	36.11	0.30	3.24	46.72	128.63	5.24	57.13	1.1453	163	0.8	4.95
119	ZS3N05	8.20	49.74	16.39	25.68	0.54	6.81	67.72	176.6	5.86	81.79	1.0245	167.5	0.72	4.2
120	ZS3N07	12.85	54.90	12.95	19.30	0.54	4.13	38.95	110.13	4.79	49.09	1.2531	161	0.9	5.7
121	ZS3N08	12.46	54.34	12.35	20.85	0.58	2.01	16.53	51.37	3.09	22.77	1.9405	153	1.05	7.2
122	ZS3N09	12.49	53.95	11.71	21.85	0.51	3.84	49.63	119	5.98	56.57	1.0027	169	0.71	4.05
123	ZS3N10	4.83	35.78	18.86	40.52	0.42	3.56	28.27	91.8	5.02	39.52	1.195	164.5	0.84	5.25
124	ZS3N11	10.07	31.84	19.46	38.63	0.42	2.3	29.24	86.24	3.78	37.76	1.5876	157	0.97	6.4
125	ZS4N01	2.63	14.02	34.40	48.95	0.87	1.51	12.18	45.06	2.66	19.22	2.2573	148.5	1.1	7.85
126	ZS4N02	3.66	14.07	31.67	50.61	0.88	4.84	38.01	108.42	5.84	48.81	1.028	168	0.73	4.3

127	ZS4N03	5.37	35.08	23.68	35.87	0.94	4.28	36.47	126.45	5.37	52.89	1.1181	166	0.78	4.85
128	ZS4N04	6.55	42.02	22.45	28.99	0.63	3.36	25.61	81.29	4.37	35.31	1.3732	162	0.92	5.95
129	ZS4N05a	5.29	14.41	29.27	51.04	0.92	2.18	25.27	121.42	3.51	46.09	1.7072	156.5	1	6.75
130	ZS4N05b	2.72	6.03	33.18	58.07	0.92	5.05	39.43	108.94	6.09	49.2	0.9855	169.5	0.68	3.8
131	ZS4N05c	3.15	8.78	31.80	56.27	0.84	3.89	39.73	99.71	5.47	46.64	1.0971	164	0.77	4.65
132	ZS4N06	13.99	43.14	17.66	25.21	0.42	4.82	39.7	111.13	5.15	50.09	1.1657	166.5	0.82	5.1
133	ZS4N07	8.15	48.48	16.96	26.41	0.89	3.08	25.58	87.18	4.26	36.81	1.4086	162.5	0.94	6.05
134	ZS4N08	3.47	9.04	30.24	57.24	0.44	1.79	20.76	70.04	2.9	29.29	2.0699	154	1.08	7.4
135	ZS4N09	7.16	27.16	31.86	42.19	0.48	4.96	43.46	120	6.02	54.2	0.9963	169	0.7	4
136	ZS4N10	7.50	22.79	23.77	45.94	0.45	5.72	75.87	271.17	5.56	110.45	1.08	167	0.75	4.55
137	ZS4N11	15.94	66.12	8.88	9.06	0.11	2.9	57.13	151.69	4.71	66.97	1.273	163	0.89	5.8
138	ZS4N12	8.80	32.35	16.93	41.92	0.17	2.2	18.38	62.56	3.38	26.59	1.7777	157.5	1.02	6.9
139	ZS4N13	9.05	41.21	15.63	34.12	0.16	5.1	39.44	107.67	6.14	49.16	0.9776	170	0.66	3.7
140	ZS5N01	1.36	45.99	22.64	30.02	0.43	4.39	36.87	107.31	5.38	47.63	1.1163	165	0.79	4.85
141	ZS5N02	1.57	35.10	24.08	39.25	0.42	3.37	43.87	144.78	5.12	60.69	1.171	166.5	0.83	5.15
142	ZS5N03	1.36	9.47	31.87	57.30	0.35	3.04	23.6	76.54	4.13	32.99	1.4512	162	0.93	6.1
143	ZS5N04	1.38	66.73	16.52	15.37	0.58	1.65	20.65	80.77	3.02	32.28	1.9869	154.5	1.07	7.3
144	ZS5N05	1.27	20.49	28.39	49.85	0.37	4.64	37.03	117.87	5.94	50.68	1.0097	169	0.71	4.1
145	ZS5N06	3.19	71.09	12.63	13.09	0.61	4.18	38.37	130.72	5.49	54.81	1.0921	167.5	0.76	4.6
146	ZS6N01	4.45	58.71	16.82	20.03	0.69	2.73	37.45	103.1	4.45	45.79	1.348	163.5	0.9	5.85
147	ZS6N02	0.89	14.74	28.31	56.07	0.45	1.87	31.63	99.05	3.36	41.68	1.7842	158	1.01	6.95
148	ZS6N03	2.34	35.47	22.03	40.16	0.30	5.02	33.11	94.15	6.1	42.88	0.984	170	0.67	3.75
149	ZS6N04	1.07	26.94	25.70	46.29	0.77	3.65	39.17	108.33	5.24	48.75	1.1444	165.5	0.8	4.95
150	ZS6N05	0.86	18.16	27.25	53.72	0.40	4.17	32.27	91.21	5.1	41.04	1.1764	167	0.84	5.2
151	ZS6N06	0.60	14.72	27.16	57.52	0.80	3.03	23.34	75.94	3.98	32.86	1.5089	162.5	0.95	6.2
152	ZS6N06b	0.68	22.91	24.93	51.48	0.54	1.82	12.04	37.15	2.87	16.89	2.0933	155	1.09	7.45

153	ZS6N06c	1.13	66.54	13.68	18.65	0.48	4.73	38.13	106.59	5.89	48.04	1.0188	169	0.72	4.15
154	ZS6N06d	1.02	69.03	12.70	17.25	0.50	3.4	51.6	122.6	5.47	57.62	1.0961	167.5	0.77	4.65
155	ZS6N06e	0.77	15.94	27.12	56.17	0.64	3.01	63.47	176.75	4.38	76.08	1.3708	163.5	0.91	5.9
156	ZS6N06f	2.81	47.04	31.86	34.39	0.26	5.35	42.23	126.02	6.22	55.61	0.9653	180	0.65	3.59
157	Kilimli 1	1.98	28.46	24.69	44.87	0.53	6.33	50.16	128.2	6.22	60.16	0.9644	180.00	0.65	3.59
158	Kilimli 2	1.62	29.69	27.02	41.67	0.59	5.09	38.73	114.05	6	50.48	0.9994	173.00	0.70	4.04
159	Kilimli 3	2.09	30.41	25.15	42.35	0.67	5.06	41.88	123.26	6.14	54.6	0.9776	186.00	0.67	3.62
160	Kilimli 4	2.25	27.11	24.46	46.18	0.51	3.72	33.09	117.31	4.94	48.54	1.2144	150.00	0.82	5.44
161	Kilimli 5	2.17	28.99	28.13	40.71	0.47	5.65	38.39	104.34	6.31	48.19	0.9514	189.00	0.66	3.47
162	Kilimli 6	1.74	37.13	22.98	38.15	0.39	4.71	41.13	143.31	5.71	59.73	1.0506	175.00	0.76	4.35
163	Kilimli 7	3.01	41.22	17.89	37.88	0.65	4.25	29.09	108.88	5.42	44.64	1.1068	172.00	0.82	4.77
164	Kilimli 8	2.62	40.10	18.52	38.76	0.60	3.94	37.78	97.43	5.4	45.23	1.1118	176.00	0.85	4.82
165	Gelik 1	2.12	25.06	26.01	46.81	0.44	4.39	62.33	167.66	6.36	75.28	0.9438	193.00	0.62	3.19
166	Gelik 2	1.88	26.05	25.15	46.92	0.36	8.87	75.34	231.51	6.43	100.3	0.9333	195.00	0.61	3.11
167	Gelik 3	1.74	23.17	26.11	48.98	0.32	5.39	39.7	109.09	6.5	49.92	0.9231	202.00	0.57	2.82
168	Gelik 4	2.62	29.32	22.57	45.49	0.47	5.61	41.65	115.41	6.47	52.38	0.9275	197.00	0.59	2.98
169	Gelik 5	2.09	24.68	28.19	45.04	0.41	5.25	37.23	103.07	6.24	47.23	0.9613	187.00	0.66	3.55
170	Gelik 6	2.42	30.27	24.45	42.86	0.33	4.61	42.89	122.61	6.4	54.87	0.9378	192.00	0.61	3.16
171	Gelik 7	1.93	26.25	27.11	44.71	0.55	80.79	64.25	149.97	6.28	73.51	0.9548	188.00	0.65	3.48
172	Gelik 8	2.76	25.81	27.84	43.59	0.62	4.43	37.07	101.76	6.31	46.61	0.9511	187.00	0.64	3.41
173	Gelik 9	1.63	24.71	28.08	45.58	0.38	3.83	29.05	93.12	4.86	40.05	1.2335	172.00	0.95	5.54
174	Gelik 10	2.29	29.14	23.66	44.91	0.47	4.44	41.94	103.47	6.08	49.23	0.9861	200.00	0.77	3.85
175	Gelik 11	2.11	28.43	22.81	46.65	0.29	4.43	41.03	118.45	5.04	52.53	1.1907	187.00	0.98	5.23
176	Gelik 12	2.38	26.17	28.37	43.08	0.51	5.4	45.38	131.44	6.45	58.43	0.9298	194.00	0.59	3.06
177	Gelik 13	2.59	25.84	26.74	44.83	0.34	4.7	43.67	104.67	6.33	50.58	0.9482	201.00	0.66	3.29
178	Gelik 14	2.07	24.79	26.92	46.22	0.58	5.36	38.07	106.55	6.32	48.52	0.9489	204.00	0.67	3.30

179	Gelik 15	2.16	25.05	29.01	43.78	0.47	4.35	61.66	168.69	6.4	75.27	0.9376	194.00	0.61	3.14
180	Gelik 16	2.47	24.89	23.39	49.25	0.32	5.65	43.74	112.74	6.44	52.86	0.931	204.00	0.63	3.07
181	Gelik 17	2.33	27.13	28.43	42.11	0.46	5.96	49.01	128.21	6.51	59.37	0.9224	197.00	0.49	2.48
182	Gelik 18	1.68	23.96	28.11	46.25	0.41	5.46	39.82	109.87	6.33	49.73	0.9475	205.00	0.66	3.22
183	Imported Steam Coal 1	4.18	11.23	32.48	52.11	0.57	4.39	37.11	122.89	5.46	52.15	1.0979	167.00	0.78	4.67
184	Imported Steam Coal 2	10.48	7.67	34.45	47.40	0.43	1.74	19.46	101.11	2.97	37.91	2.0195	147.00	1.08	7.35
185	Imported Steam Coal 3	12.48	4.83	34.92	47.77	0.40	1.33	12.81	63.98	2.52	25.55	2.3779	147.00	1.18	8.03
186	Imported Steam Coal 4	4.50	11.99	21.94	61.57	0.32	5.07	38.49	116.11	6.15	51.04	0.9751	174.00	0.63	3.62
187	Imported Steam Coal 5	3.94	12.61	31.37	52.08	0.88	4.9	35.25	102.34	6.04	45.93	0.9939	175.00	0.70	4.00
188	Imported Steam Coal 6	8.96	12.15	27.89	51.00	0.39	3.28	57.46	137.71	5.42	64.32	1.108	166.00	0.80	4.82
189	Imported Steam Coal 7	8.85	11.52	25.40	54.23	0.36	3.31	21.4	63.34	4.46	28.57	1.3447	159.00	0.93	5.85
190	Imported Steam Coal 8	10.45	10.07	30.18	49.30	0.39	2.45	32.47	92.38	3.97	40.71	1.5101	152.00	0.95	6.25
191	Imported Steam Coal 9	10.66	9.61	30.66	49.07	0.44	3.16	31.09	80.38	4.49	37.04	1.3358	149.00	0.87	5.84
192	Imported Steam Coal 10	9.92	9.72	30.10	50.26	0.49	3.24	22.02	80.82	4.3	33.45	1.3943	153.00	0.92	6.01
193	Imported Steam Coal 11	10.17	9.65	30.12	50.06	0.40	4	35.01	153.32	4.08	63.64	1.469	153.00	0.94	6.14
194	Imported Steam Coal 12	9.95	8.53	31.05	50.47	0.35	2.76	23.27	80.65	3.83	33.96	1.5685	152.00	0.97	6.38
195	Imported Steam Coal 13	11.04	8.77	30.10	50.09	0.34	2.85	20.59	68.4	3.83	29.09	1.5665	151.00	0.96	6.36
196	Imported Steam Coal 14	8.92	9.45	30.12	51.51	0.36	3.57	32.24	100.12	4.78	43.2	1.2553	156.00	0.89	5.71
197	Imported Steam Coal 15	9.91	10.80	30.19	49.08	0.46	2.99	22.37	82.97	4.17	34.31	1.4402	153.00	0.93	6.08
198	Imported Steam Coal 16	9.89	10.12	30.08	49.91	2.12	3.25	27.87	85.86	4.17	37.59	1.4376	153.00	0.93	6.08
199	Imported Steam Coal 17	9.03	10.75	30.30	49.92	0.38	3.57	29.49	104.67	4.69	43.49	1.2802	155.00	0.90	5.81
200	Imported Steam Coal 18	9.70	11.29	30.32	48.69	0.39	3.27	36.99	129.19	4.91	53.49	1.222	154.00	0.84	5.45
201	Imported Steam Coal 19	9.27	10.85	30.46	49.42	0.32	3.21	21.67	67.38	4.5	29.82	1.3346	156.00	0.91	5.83
202	Imported Steam Coal 20	9.61	9.73	30.23	50.43	0.27	3.2	21.24	77.97	4.35	32.69	1.3807	154.00	0.92	5.97
203	Imported Steam Coal 21	8.85	9.78	30.63	50.74	0.30	3.73	34.96	106.21	4.74	46.23	1.2663	157.00	0.90	5.73
204	Imported Steam Coal 22	9.55	9.95	30.63	49.87	0.39	3.05	22.96	86.7	4.36	35.37	1.3775	154.00	0.92	5.97

205	Imported Steam Coal 23	8.95	9.41	30.80	50.84	0.36	3.77	25.45	76.78	4.7	34.36	1.2778	155.00	0.90	5.81
206	Imported Steam Coal 24	9.00	10.78	30.39	49.83	0.38	2.88	35.38	96.41	4.7	43.26	1.2778	155.00	0.90	5.81
207	Imported Steam Coal 25	10.00	10.75	30.68	48.57	0.36	2.69	27.21	83.43	4.09	36.36	1.4675	153.00	0.94	6.14
208	Imported Steam Coal 26	9.94	11.39	30.50	48.17	0.44	2.88	20.29	62.02	3.88	27.23	1.548	154.00	0.97	6.30
209	Imported Steam Coal 27	9.02	10.14	31.46	49.38	0.31	2.56	53.76	157.13	4.57	67.39	1.3142	156.00	0.91	5.83
210	Imported Steam Coal 28	8.70	11.17	30.74	49.39	0.37	3.76	23.85	75.16	4.79	33.15	1.2522	157.00	0.89	5.67
211	Imported Steam Coal 29	9.02	10.76	30.65	49.57	0.39	3.11	52.36	181.11	4.7	73.98	1.276	155.00	0.90	5.81
212	Imported Steam Coal 30	10.76	7.92	30.89	50.43	0.31	2.61	21.12	70.17	3.73	29.71	1.6071	151.00	0.97	6.42
213	Imported Steam Coal 31	10.29	10.66	30.42	48.63	0.48	2.52	27.98	90.18	4	38.27	1.5018	152.00	0.94	6.18
214	Imported Steam Coal 32	9.51	11.08	30.42	48.99	0.38	3.32	24.33	83.25	4.37	35.45	1.3744	154.00	0.92	5.97
215	Imported Steam Coal 33	10.84	9.78	30.35	49.03	0.41	2.62	29.3	84.13	3.68	37.11	1.6311	149.00	0.96	6.44
216	Imported Steam Coal 34	9.84	10.17	30.63	49.36	0.32	3.05	20.82	68.3	4.18	29.76	1.4362	153.00	0.93	6.08

652

653

References

[1]. Arisoy, A., & Beamish, B. B. (2015). Mutual effects of pyrite and moisture on coal self-heating rates and reaction rate data for pyrite oxidation. Fuel, 139, 107–114. https://doi.org/10.1016/j.fuel.2014.08.036

[2]. Bilen, M. (2025). Online CO Monitoring During Low Temperature Oxidation of Zonguldak Coals. Combustion Science and Technology, 197(15), 4011–4029. https://doi.org/10.1080/00102202.2024.2359619

[3]. Bilen, M., Yılmaz, S., & Barış, K. (2026). An Integrated Color Space–Thermochemical Framework for Predicting Coal Spontaneous Combustion Liability. Combustion Science and Technology, 1–28. https://doi.org/10.1080/00102202.2026.2687003

[4]. Choi H, Thiruppathiraja C, Kim S et al (2011) Moisture readsorption and low temperature oxidation characteristics of upgraded low rank coal. Fuel Process Technol 92:2005–2001. https://doi.org/10.1016/j.fuproc.2011.05.025

[5]. Deng J, Xiao Y, Li Q et al (2015) Experimental studies of spontaneous combustion and anaerobic cooling of coal. Fuel 157:261–269. https://doi.org/10.1016/j.fuel.2015.04.063

[6]. Deng J, Yang Y, Zhang YN, Liu B, Shu CM. Inhibiting effects of three commercial inhibitors in spontaneous coal combustion. Energy 2018. https://doi.org/10.1016/ j.energy.2018.07.040.

[7]. Deng J, Zhang Y, Zhao J et al (2019) Experiment study on oxidation and activated energy of different partical size coal based on programmed temperature rising. Coal Sci Technol 47(1):214–219

[8]. Du W, Zhang J, Xie Q et al (2020) Experimental study on optimizing the inhibition effect of pre-injection inhibitor on coal spontaneous combustion. Energy Sources, Part A Recover Util Environ Eff. https://doi.org/10.1080/15567036.2020.1780350

[9]. Du W, Zhang J, Xie Q et al (2020) Experimental study on optimizing the inhibition effect of pre-injection inhibitor on coal spontaneous combustion. Energy Sources, Part A Recover Util Environ Eff. https://doi.org/10.1080/15567036.2020.1780350

[10]. Du, B., Liang, Y., Tian, F., & Guo, B. (2023). Analytical Prediction of Coal Spontaneous Combustion Tendency: Pore Structure and Air Permeability. Sustainability, 15(5), 4332. https://doi.org/10.3390/su15054332

[11]. Feng KK, Chakravorty RN, Cochrane TS. 1973 Oct. Spontaneous combustion: A coal mining hazard. Can Min Metall Bull. 66(738):75–84.

[12]. Jia, X., Wu, J., Lian, C. et al. Investigating the effect of coal particle size on spontaneous combustion and oxidation characteristics of coal. Environ Sci Pollut Res 29, 16113–16122 (2022). https://doi.org/10.1007/s11356-021-16929-1

[13]. Jiang, X., Li, J., & Qiu, J. (1999). The influence of particle size on composition analyzing and combustion characteristics of pulverized coal. Mei T'an Hsueh Pao (Journal of China Coal Society), 24.

[14]. Kong B, Wang E, Lu W, Li Z (2019) Application of electromagnetic radiation detection in high-temperature anomalous areas experiencing coalfield fires. Energy 189:116144. https://doi.org/10.1016/j. energy. 2019. 116144

[15]. Küçük, A., Kadıoğlu, Y., & Gülaboğlu, M.Ş. (2003). A study of spontaneous combustion characteristics of a Turkish lignite: Particle size, moisture of coal, humidity of air. *Combustion and Flame, 133*(3), 255–261. https://doi.org/10.1016/S0010-2180(02)00553-9

[16]. Li X, Choi M, Kim K et al (2019) Effects of pulverized coal particle size on flame structure in a methane-assisted swirl burner. Fuel 242:68–76. https:// doi. org/ 10. 1016/j. fuel. 2019. 01. 009

[17]. Li B, Li M, Gao W, Mingshu B, Ma L, Qin Q, et al. Effects of particle size on the self-ignition behaviour of a coal dust layer on a hot plate. Fuel 2020;260(Jan). https://doi.org/10.1016/j.fuel.2019.116269

[18]. Ma L, Guo R, Gao Y, Ren L, Wei G, Li C. Study on coal spontaneous combustion characteristics under methane-containing atmosphere. Combust Sci Technol 2018. https://doi.org/10.1080/00102202.2018.1531286.

[19]. Mishra, D. P. (2022). Effects of intrinsic properties, particle size and specific surface area on WOP and spontaneous combustion susceptibility of coal. *Advanced Powder Technology, 33*(3), 103454. https://doi.org/10.1016/j.apt.2022.103454

[20]. Mishra, Debashish; Mishra, D.P.; Mohalik, N K; Ray, S K; and Pandey, J K (2025) "Effect of depth and particle size on spontaneous combustion of coal in deep underground mines of Jharia coalfield," Journal of Sustainable Mining: Vol. 24 : Iss. 1 , Article 7. https://doi.org/10.46873/2300-3960.1443

[21]. Nugroho YS, McIntosh AC, Gibbs BM (2000) Low-temperature oxidation of single and blended coals. Fuel 79:1951–1961. https:// doi. org/ 10. 1016/ S0016-2361(00) 00053-3

[22]. Onifade M, Genc B. A review of research on spontaneous combustion of coal. Int J Min Sci Technol 2020;30(3):303–11. https://doi.org/10.1016/j.ijmst.2020.03.001.

[23]. Qin, Y.P., Song, Y.M., and Yang, X.B.. (2010). Experimental study on coal granularity influencing oxidation rate in goaf. Journal of China Coal Society, 35(S1), 132-135.

[24]. Qin Y, Liu W, Yang C, Fan Z, Wang L, Jia G. Experimental study on oxygen consumption rate of residual coal in goaf. Saf Sci 2012. https://doi.org/10.1016/j.ssci.2011.08.033.

[25]. Qin Y, Song Y, Liu W et al (2020) Assessment of low-temperature oxidation characteristics of coal based on standard oxygen consumption rate. Process Saf Environ Prot 135:342–349. https://doi.org/10.1016/j.psep. 2019.12.039

[26]. Song J, Deng J, Zhao J et al (2021) Critical particle size analysis of gas emission under high-temperature oxidation of weathered coal. Energy 214:118995. https:// doi. org/ 10. 1016/j. energy. 2020. 118995

[27]. Song JJ, Deng J, Zhao JY et al (2021) Comparative analysis of exothermic behaviour of fresh and weathered coal during low-temperature oxidation. Fuel 289:119942. https:// doi. org/ 10. 1016/j. fuel. 2020.119942

[28]. Yong S, Shugang W, Lu W, Cao Y jiazi, Li J. Coal spontaneous combustion characteristics based on constant temperature difference guidance method. Process Saf Environ Protect 2019. https://doi.org/10.1016/j.psep.2019.09.013.

[29]. Taraba B, Michalec Z, Michalcov´a V, Blejcha˘r T, Bojko M, Kozubkov´a M. CFD simulations of the effect of wind on the spontaneous heating of coal stockpiles. Fuel 2014. https://doi.org/10.1016/j.fuel.2013.10.064.

[30]. Wang, C., Yang, Y., Tsai, YT. et al. Spontaneous combustion in six types of coal by using the simultaneous thermal analysis-Fourier transform infrared spectroscopy technique. J Therm Anal Calorim 126, 1591–1602 (2016). https://doi.org/10.1007/s10973-016-5685-2

[31]. Wang CP, Zhao XY, Bai ZJ, et al (2021) Comprehensive index evaluation of the spontaneous combustion capability of different ranks of coal. Fuel 291:. https:// doi. org/ 10. 1016/j. fuel. 2020. 120087

[32]. Wang, Q., Lu, X., Ma, C. et al. Comparative study of the kinetic characteristics of coal spontaneous combustion. J Therm Anal Calorim 148, 4463–4476 (2023). https://doi.org/10.1007/s10973-023-12028-0

[33]. Wen H, Yu Z, Deng J, Zhai X. Spontaneous ignition characteristics of coal in a large-scale furnace: an experimental and numerical investigation. Appl Therm Eng 2017. https://doi.org/10.1016/j.applthermaleng.2016.12.022.

[34]. Wolf KH, Bruining H. Modelling the interaction between underground coal fires and their roof rocks. Fuel 2007. https://doi.org/10.1016/j.fuel.2007.03.009.

[35]. Xu Q, Yang S, Yang W et al (2021) Effect of particle size and low-temperature secondary oxidation on the active groups in coal structures. Process Saf Environ Prot 149:334–344. https://doi.org/10.1016/j.psep.2020.10.056

[36]. Yang, F., Lai, Y., & Song, Y. (2019). Determination of the influence of pyrite on coal spontaneous combustion by thermodynamics analysis. Process Safety and Environmental Protection, 129, 163–167. https://doi.org/10.1016/j.psep.2019.06.023

[37]. Yang Y, Li Z, Si L, Hou S, Li Z, Li J. Study on test method of heat release intensity and thermophysical parameters of loose coal. Fuel 2018. https://doi.org/10.1016/j.fuel.2018.05.006.

[38]. Yilmaz, S., 2019. A new approach for the testing method of coal grindability. *Advanced Powder Technology*, 30(9), pp.1932–1940. https://doi.org/10.1016/j.apt.2019.06.012.

[39]. Yilmaz, S. (2025). Prediction of spontaneous combustion liability for imported steam coals. Energy Sources, Part A: Recovery, Utilization, and Environmental Effects, 47(1), 12329–12343. https://doi.org/10.1080/15567036.2025.2512224

[40]. Yu M, Ma S, Chu T (2016) Influence study of coal particle size on the gases production rule and spontaneous combustion tendency characteristics. J Henan Polytech Univ 38:25–31

[41]. Zhang C, Zhang L (2019) Permeability Characteristics of Broken Coal and Rock Under Cyclic Loading and Unloading. Nat Resour Res 28:1055–1069. https://doi.org/10.1007/s11053-018-9436-x

[42]. Zhang YT, Zhang XC, Tien JC, Li YQ (2011) Evaluation of the propensity for coal spontaneous combustion based on catastrophe theory. J Coal Sci Eng 17:265–269. https://doi.org/10.1007/s12404-011-0307-x

[43]. Zhang, L., Aziz, N., Ren, T., Nemcik, J., & Tu, S. (2014). Influence of coal particle size on coal adsorption and desorption characteristics. Arch Min Sci, 59 (3) (2014), pp. 807-820

[44]. Zhang Y, Chen L, Zhao J et al (2019) Evaluation of the spontaneous combustion characteristics of coal of different metamorphic degrees based on a temperature-programmed oil bath experimental system. J Loss Prev Process Ind 60:17–27. https://doi.org/10.1016/j.jlp.2019.03.007

[45]. Zhao J, Deng J, Song J, Shu CM (2019) Effectiveness of a high-temperature-programmed experimental system in simulating particle size effects on hazardous gas emissions in bituminous coal. Saf Sci 115:353–361. https://doi.org/10.1016/j.ssci.2019.02.008

[46]. Zhou L, Dai G, Qin R et al (2020) Comprehensive risk evaluation of coal spontaneous combustion in goafs based on systems-theoretic accident model and processes. Geomatics, Nat Hazards Risk 11:1565–1580. https://doi.org/10.1080/19475705.2020.1805032